Dynamic Testing of a High-Specific-Torque Concentric Magnetic Gear

Justin J. Scheidler
Research Engineer

Zachary A. Cameron
Research Engineer

Thomas F. Tallerico
Research Engineer

NASA Glenn Research Center
Cleveland, OH, USA

ABSTRACT

This paper presents measurements of the efficiency of NASA's 2nd magnetic gear prototype. A detailed discussion of the test rig used to make these measurements was presented, including a thorough uncertainty analysis. The reported uncertainties are 95% confidence intervals that include the effects of temperature and parasitic loads. The prototype's response was measured at output speeds between 124 rpm and 744 rpm for a controlled output torque of 10 Nm (8% of the prototype's maximum torque). After correcting for tare losses, the prototype's efficiency was found to decrease from 90.0% to 83.0% as speed increased. If the efficiency is extrapolated to a typical operating condition (85% of maximum torque) using the good assumption that energy loss is approximately independent of the transmitted torque, the expected efficiency would be 99.0% to 98.4%, which exceeds the state of the art for these speeds.

INTRODUCTION

Gearing is critically important for the drivetrains of conventional vertical lift aircraft, because it provides a mechanical advantage. This advantage enables high speed, relatively low torque gas turbine engines to drive large rotors that demand low speed, high torque excitations. Most future electrified aircraft will also benefit from using gearing, either for the aforementioned reason or for improving the overall efficiency of drivetrains composed of electric-motor-driven rotors. Large fans that slowly rotate at higher torque more efficiently produce thrust (Refs. 1, 2), but electric motors are most efficient when they spin fast and produce lower torque (Refs. 2–4). Even electrified aircraft that employ many smaller rotors spinning at moderate speeds (about 2,000 rpm to 8,000 rpm) can be better optimized in terms of mass and efficiency by using gearing; high speed motors are often most efficient at speeds of 10,000 rpm to 20,000+ rpm and fast motors also tend to be smaller, which reduces the motor's impact on airflow behind the rotor.

Mechanical gearing can satisfy the gearing needs of future electrified aircraft by providing a mature technology with high to very high efficiency (99% to >99.5% per gear stage (Refs. 5,6)) and specific torque (torque/mass). However, their performance comes at the expense of lubrication requirements as well as routine and costly maintenance to monitor and prevent contact-related tooth wear and crack initiation. Due to their relatively short missions (Ref. 7) and need to traverse a more crowded and urban airspace, which will lead to more frequent use of maneuvers and hover, the time between gearbox maintenance will likely be shorter for urban air mobility aircraft compared to conventional rotorcraft. For many electrified aircraft, particularly ones that utilize several electric motors, these penalties will likely outweigh the benefits of using gearing. As a result, these aircraft will use a less optimal solution – a direct drive configuration (e.g., motors directly connected to the rotors and rotating at the same speed).

Magnetic gearing is a developing technology that provides a gear ratio without using physical contact to transmit torque between gears. Accordingly, magnetic gears enable the optimization of electrified aircraft drivetrains without the penalties associated with physical contact in mechanical gears. However, magnetic gearing has a low technology readiness level for aeronautics applications. Prior work by the authors has demonstrated that it is feasible for concentric magnetic gearing to match the specific torque of aerospace-grade mechanical gearing (Refs. 8, 9). Additional research is needed to evaluate and demonstrate the capability of the technology to *simultaneously* achieve the high efficiency and high specific torque that is required for aeronautics applications. To help address that need, this paper presents measurements of the efficiency of a concentric magnetic gear prototype that has state-of-the-art specific torque (NASA's 2nd magnetic gear prototype, named PT-2). These measurements will serve as a baseline for future prototypes that are specifically designed to achieve both high specific torque and high efficiency.

To date, at least sixteen papers have reported an efficiency measurement of a concentric magnetic gear (Ref. 10). All but one of those prototypes were tested at low output speeds (below 200 rpm) and the outlier was only tested up to a moderate output speed (905 rpm). Additionally, many references don't contain any information on the test rig, its measurement hardware, or data processing; of the references that do mention some of these topics, none provide a detailed discussion. These details become particularly important when testing magnetic gears that can operate at high speeds with high

Presented at the Vertical Flight Society 75th Annual Forum & Technology Display, Philadelphia, Pennsylvania, May 13–16, 2019.

efficiency, such as NASA's PT-2 tested herein.

This paper presents initial measurements of the efficiency of PT-2, which was designed for optimal specific torque at a given radius. First, a thorough description of the test rig and the measurement uncertainty is presented. Then, the data processing is explained. Finally, the measurements are presented and discussed.

E-DRIVES RIG

This section describes the test rig at the NASA Glenn Research Center – the E-Drives Rig – that was used to experimentally study the efficiency of PT-2. First, an overview of the test rig and its specifications is presented. Then, an uncertainty analysis of the rig's measurements is discussed. A more detailed description of the rig is provided in a previous publication (Ref. 9). This paper presents a summarized description along with a considerably updated uncertainty analysis.

Overview and Specifications

The E-Drives Rig was designed to study the components of an electrified drivetrain, including co-axial magnetic gears and electric motors. It is a 30 kW (40.2 hp) rotating system driven by an induction motor and loaded by an eddy current dynamometer. Figure 1 shows an image of the test rig with PT-2 installed. The E-Drives Rig was designed to provide three specialized features: very high precision, dynamic measurement, and adaptability.

The primary performance metric of interest is the efficiency of the test article, which in some cases is expected to approach 99.8% for relevant operating conditions. To properly evaluate such test articles, the measurements need to be precise enough to permit an efficiency uncertainty below $\pm 0.2\%$. The E-Drives Rig uses the most precise torque transducers comercially available to directly determine the mechanical efficiency of a gearbox. The following section demonstrates that this enables the desired precision.

Another intended use of the test rig is to study the vibration and transient response of electrified drivetrain components. This is achieved through hardware selection and structural design. The selected measurement hardware provides a bandwidth of 6 kHz. Couplings and shafts were selected or designed to be as lightweight and stiff as possible. The couplings were also chosen to eliminate backlash and minimize the reaction forces on the drivetrain due to misalignment. Additionally, the components are installed on a vibration isolation table to reduce extraneous vibration. This table's fine bolt pattern also provides adaptability so that a wide range of test articles can be evaluated.

The primary specifications of the E-Drives Rig are given in Table 1. The specifications labeled input and output denote the minimum capability of all the components on the input and output sides, respectively, of the gearbox under test.

Table 1: Key specifications of NASA's E-Drives Rig when studying gearboxes.

Test article	Max. OD, cm (in)	35.6 (14)
	Max. axial length, cm (in)	30.5 (12)
Input	Max. contin. torque, Nm (ft-lb)	12 (8.9)
	Max. speed, rpm	22,000
	Max. contin. power, kW (hp)	30 (40.2)
Output	Max. contin. torque, Nm (ft-lb)	100 (73.7)
	Max. speed, rpm	15,000[a]
	Max. contin. power, kW (hp)	30 (40.2)
	Measurement bandwidth, kHz	6

[a] With minor balancing.

Uncertainty Analysis

A rigorous uncertainty analysis was conducted for the E-Drives Rig to provide support for the experimental observations and satisfy the need for reliable data to validate efficiency models of magnetic gears. The uncertainties are derived in the Appendix, which also contains a complete list of the error specifications for the torque transducers used in the E-Drives Rig. In this section, the uncertainty analysis method is summarized and a characterization of the E-Drives Rig's uncertainty is presented.

The derived uncertainties are confidence intervals, meaning that the uncertainties reported here are valid for a selected percentage of all of the transducers produced by the manufacturer. The analysis in this work uses a confidence level of 95%, which is standard practice for uncertainty analysis (Ref. 11). The E-Drives Rig uses torque transducers that provide torque, speed, and power measurements. The uncertainty of each of these quantities is only governed by the transducer's resolution and instrument error for that output quantity. The uncertainty of these outputs is calculated according to the manufacturer's guidelines except for a small modification that allows for the inclusion of the resolution error. The modification leads to small, but essentially negligible increases in uncertainty.

The uncertainty of the measured torques in the E-Drives Rig is a function of only the torque magnitude and the transducer's temperature relative to the temperature at which it was calibrated, assuming that parasitic loads are negligible. Figure 2 depicts the torque uncertainty for both of the rig's torque transducers, which have a 100 Nm (73.7 ft-lb) rating. The uncertainty increases as the transducer shifts away from the calibration temperature. At the calibration temperature, the uncertainty varies from less than $\pm 0.012\%$ to about $\pm 0.019\%$. The torque uncertainty should stay below $\pm 0.03\%$ for most tests, because the transducers are separated from the primary heat source (the magnetic gear under test) and there is a considerable amount of thermal mass and surface area to absorb and dissipate the low to moderate heat produced by the rig's high speed bearings. The jumps in uncertainty result from the transducers' linearity and hysteresis error, which is specified by a smaller limit when the torque is kept either below 20% or below 60% of the transducer's rated torque during a test.

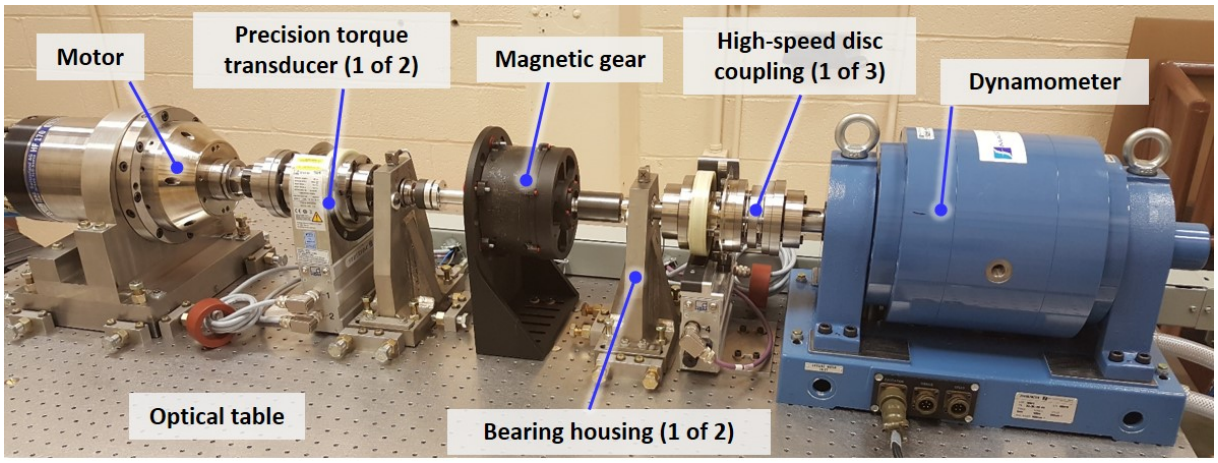

Fig. 1: E-Drives Rig at the NASA Glenn Research Center shown with NASA's 2nd magnetic gear prototype installed.

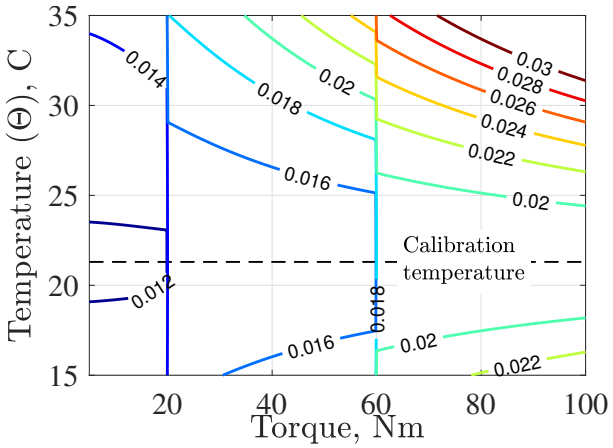

Fig. 2: Torque uncertainty (in units of Nm or % of full scale) of both of the E-Drives Rig's torque transducers measured from the CAN bus output, assuming negligible parasitic loads ($C_{\text{load}} = 0$); $T_{\text{rated}} = 100$ Nm, $T_{\text{range}} = 100$ Nm.

The key performance metric that is considered in this work is the efficiency of the magnetic gear. The efficiency is a calculated quantity that, due to error propagation, has a higher uncertainty than the measured quantities with which it is calculated. The effect of the error propagation depends on the operating condition. Consequently, the uncertainty of the calculated efficiency is dependent on the gear ratio and output speed and torque of the gear being tested. Also, the uncertainty in efficiency varies more throughout the rig's operating space than the uncertainty in quantities that are directly measured.

When the input and output power are calculated from the measure torque and speed signals, error propagation also impacts the power uncertainties. The uncertainty in the input and output power are shown in Fig. 3. For these quantities, the uncertainty depends on the speed and torque at either the input and output side of the magnetic gear. Thus, the depicted uncertainty of the input power depends on the gear ratio of the magnetic gear under test, because the results are shown for a consistent region of the operating space. For each of the powers, two different uncertainties are given: one for when the power is calculated from the measured torque and speed and another for when the power is directly measured. The power uncertainty is typically smaller for the directly measured powers, but the uncertainty in the calculated power is lower when the speed and torque are low.

The efficiency uncertainty for testing the prototypes considered in this paper is presented in Fig. 4. At low speeds and, in one of the cases, at low torques, the uncertainty can exceed $\pm 0.5\%$. However, over most of the operating space, the efficiency can be calculated to within $\pm 0.2\%$ with a 95% confidence level. This is important for verifying that a high efficiency magnetic gear actually achieves its performance target.

For all of the results shown in this paper, the uncertainty analysis described above and in the Appendix is used to overlay a 95% confidence interval on top of each data point.

MEASUREMENTS

The rig's two torque transducers are separated from one another by not only the test article, but also two bearing housings, a flexible coupling, a rigid coupling, and two shaft clamps. This decision was made due to constraints on where the test rig's torque transducers can be located and a desire to isolate them from the test article (for thermal, vibration, and safety reasons). Consequently, the power loss and efficiency calculated from the measurements include bearing losses and the windage loss associated with those rotating components.

To account for this, the tare losses were directly measured when a simple straight shaft was installed in place of a test article. In this operating condition, the input and output sides of the rig rotate at the same speed and, thus, contribute essentially equally to the total measured power loss. When testing a gearbox, there is a potentially large difference between the rig's losses on its input and output sides due to the potentially large difference in speed. To account for this discrepancy, it was assumed that the input and output sides contribute equally to the measured tare loss. This is considered a good assumption, because bearing losses dominate the tare loss and the

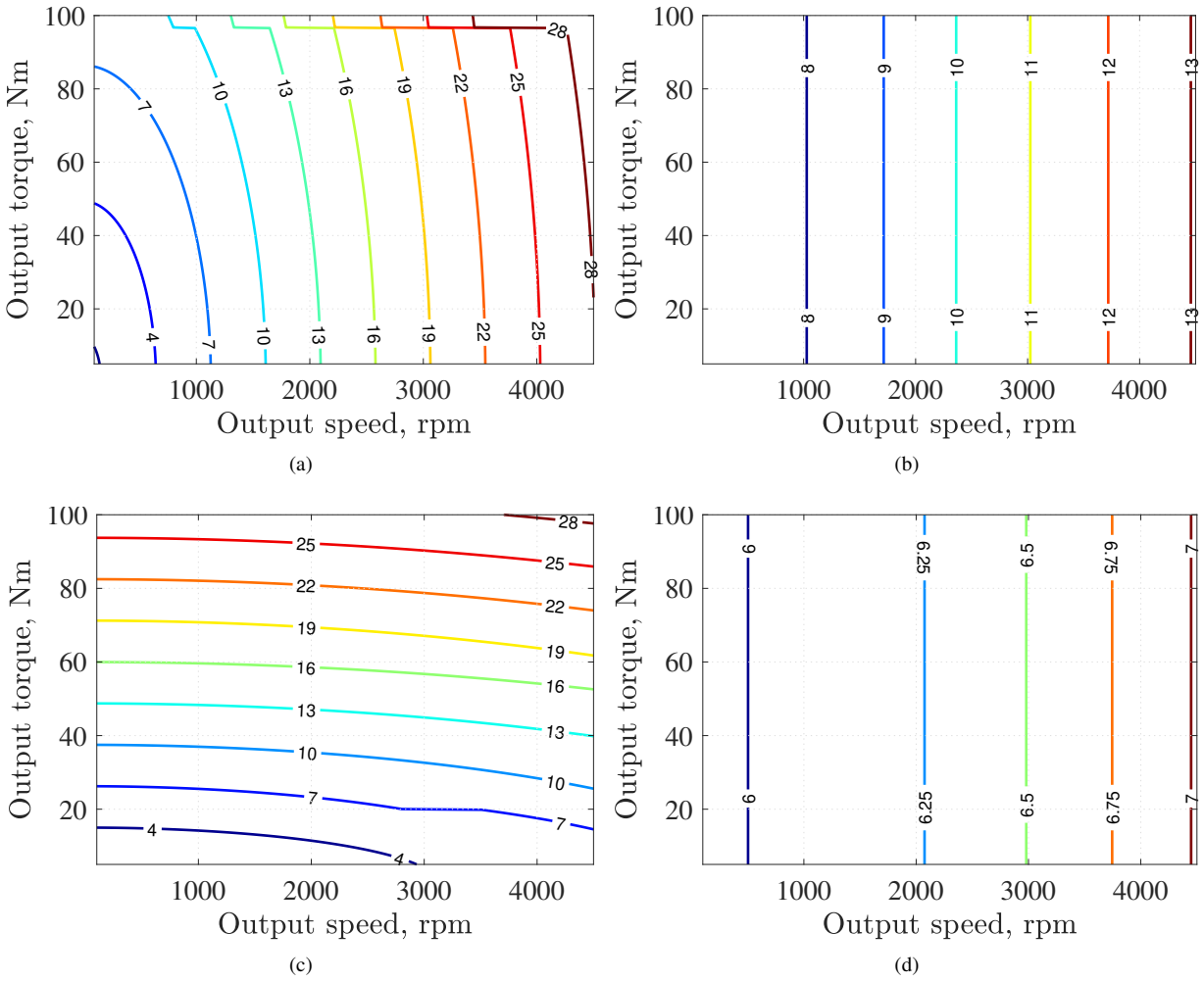

Fig. 3: Uncertainty (in units of W) in the input power ((a),(b)) and output power ((c),(d)) for testing a magnetic gear with gear ratio of 4.83 in the E-Drives Rig, when the power is (a),(c) calculated from measured torque and speed CAN bus signals or (b),(d) directly measured; assuming negligible parasitic loads ($C_{\text{load}} = 0$) and a conservative estimate of the transducer's temperature during testing (10 °C above calibration temperature); $T_{\text{rated}} = 100$ Nm, $T_{\text{range}} = 100$ Nm.

only asymmetry in the test rig is the very small difference in windage losses between the flexible coupling (on the input side) and the rigid coupling (on the output side). With this assumption, the tare loss on the input and output sides of the E-Drives Rig can be quantified as a function of speed so that the total tare loss during a magnetic gear test can be calculated from the input and output speeds. The measured tare losses are shown in Fig. 5. The tare loss is well fit by a power law, which was used to calculate the tare loss that occurred during a magnetic gear test. To gain more confidence in the tare loss calculation (i.e., reduce uncertainty), the tare loss can be measured again in the future at a higher load torque and using the power output from the torque transducers.

NASA's 2nd magnetic gear prototype

Although PT-2 was designed to achieve a high specific torque rather than a high efficiency, the intention of this test was to evaluate the efficiency of the prototype over a subset of its operating space to compare to the existing state of the art and to establish a baseline for future prototypes that implement features for improving efficiency. A limited amount of testing of this prototype was completed before testing had to be stopped due to damage to the modulator, which is the rotor containing soft magnetic materials that allow the sun and ring gears' magnet arrays to interact. The damage, which is discussed in detail elsewhere (Ref. 12), resulted from a flaw in the modulator's fabrication that allowed some of the pole piece laminations to be pulled out of the modulator.

The prototype's response was measured at output speeds between 124 rpm and 744 rpm for a controlled output torque of 10 Nm (7.38 ft-lb). Figure 6 presents the average efficiency of the prototype after correcting the data by subtracting the tare loss. The measured efficiency decreases from 90.0% to 83.0% as the speed increases. For comparison, the inefficiency due to the tare loss increased from 1.25% to 1.55% over the same span. Thus, small errors in the quantification of the tare loss would have a negligible effect. The output

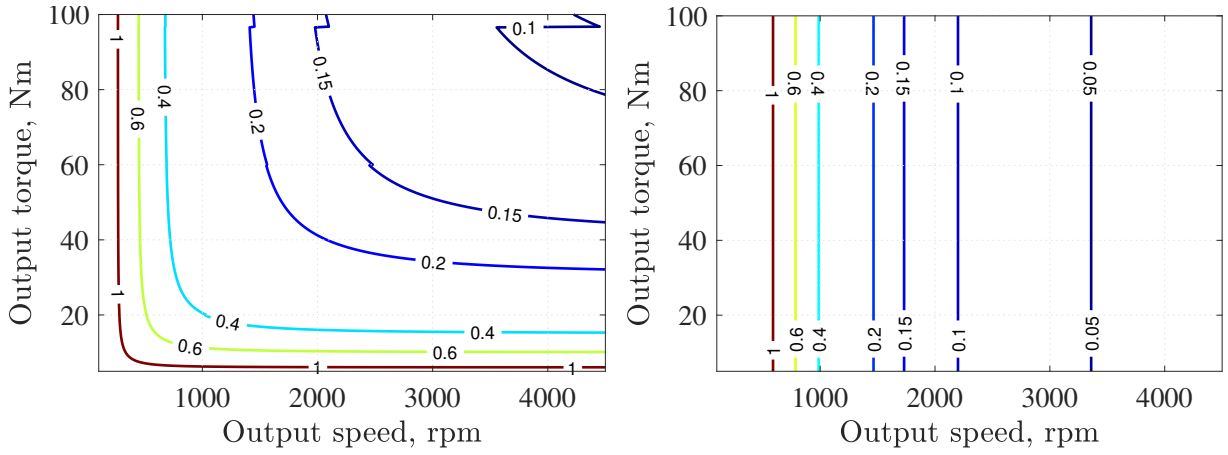

Fig. 4: Uncertainty in the efficiency (in units of %) for testing a magnetic gear with gear ratio of 4.83 in the E-Drives Rig, for power (a) calculated from measured torque and speed CAN bus signals and (b) directly measured; assuming negligible parasitic loads ($C_{\text{load}} = 0$) and a conservative estimate of the transducer's temperature during testing (10 °C above calibration temperature); $T_{\text{rated}} = 100$ Nm, $T_{\text{range}} = 100$ Nm.

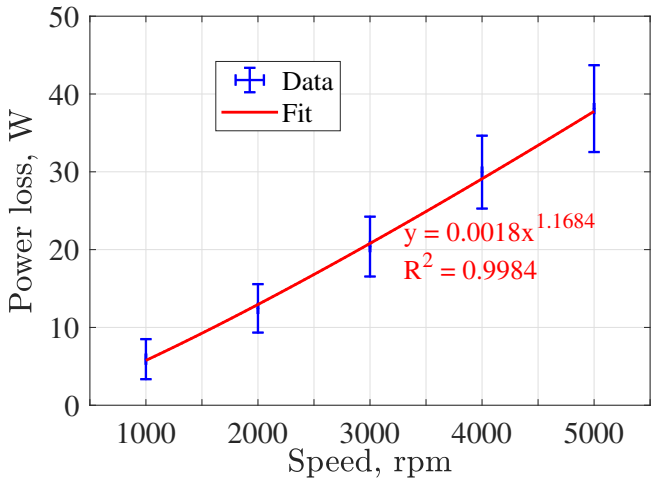

Fig. 5: Tare loss in the E-Drives Rig when a simple straight shaft was installed in place of a test article, for a load torque of 5 Nm (3.69 ft-lb); calculated from measured torques and speeds; 95% confidence intervals depicted.

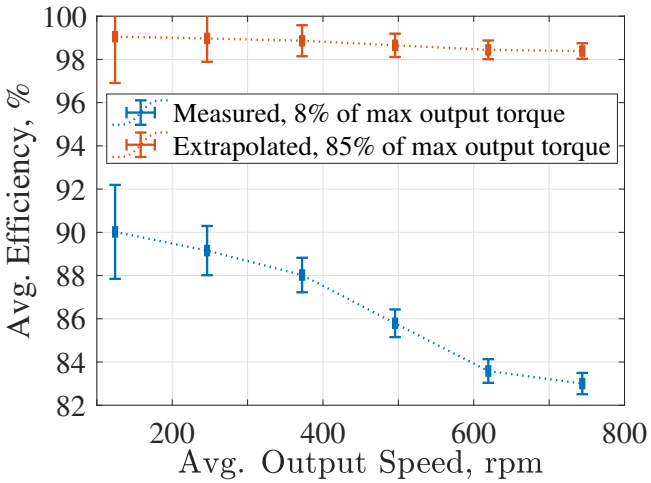

Fig. 6: Corrected average efficiency of NASA's 2nd magnetic gear prototype, measured at 8% of the prototype's maximum output torque and extrapolated to 85% of its maximum output torque by assuming that the losses are torque independent; 95% confidence intervals depicted.

torque during this test is only 8% of the prototype's pullout torque (124 Nm (91.5 ft-lb)). It has been demonstrated that the energy loss in a concentric magnetic gear is approximately independent of the transmitted torque (Refs. 13–15); as a result, the efficiency of a concentric magnetic gear increases monotonically with the output torque (and thus the transmitted power). Consequently, the measured efficiency can be extrapolated to determine the approximate efficiency at a higher torque. It is common to define the rated torque of a magnetic gear as 85% of the pullout torque. Figure 6 also depicts the extrapolated average efficiency of the prototype at 85% of the pullout torque. In that operating condition, the expected efficiency is 99.0% to 98.4%. This efficiency exceeds the state of the art over this speed range.

CONCLUSIONS

This paper presented initial measurements of the efficiency of NASA's 2nd magnetic gear prototype (PT-2). A detailed discussion of the test rig's design and capabilities was presented. Testing is conducted on the E-Drives Rig, which was recently commissioned at the NASA Glenn Research Center. To address the need for high precision data for model validation and to enable reliable measurement of very high efficiencies, a thorough uncertainty analysis was conducted. The reported uncertainties are 95% confidence intervals that include the effects of temperature and parasitic loads. The uncertainty analysis indicates that in the E-Drives Rig torque can be measured to better than ±0.02% uncertainty if the torque transducers'

temperature is tightly controlled and to better than ±0.03% uncertainty for most tests that don't have temperature control. Using a conservative estimate for the transducers' temperature rise experienced in this experiment, the mechanical efficiency of the test gearbox can be calculated to within ±0.2% over most of the operating space and to within ±0.05% at higher speeds. However, the efficiency data reported in this paper has an uncertainty that varies from ±2% to about ±0.25%, because the measurements were obtained at low torque and low to moderate speeds.

A discussion was presented of post processing the data to correct for the rig's tare losses that are generated in the rig's bearings (due to friction) and on the rig's rotating components (due to windage). The tare loss was measured at low torque and a range of speeds after the test article was replaced by a simple straight shaft. While testing PT-2, an existing flaw in the modulator was damaged further, causing a premature stop to testing. The response was measured at output speeds between 124 rpm and 744 rpm for a controlled output torque of 10 Nm. The inefficiency due to the tare loss ranged from 1.25% to 1.55%, which is small compared to the corrected efficiency of PT-2 (90.0% to 83.0% over the same span). Thus, small errors that may have occurred in quantifying the tare loss would have a negligible effect on the corrected efficiency. In absolute terms, the measured efficiency is low. However, it was achieved at torque that is only 8% of the prototype's maximum (124 Nm). If the efficiency is extrapolated to a typical operating condition (85% of maximum torque) using the good assumption that energy loss is approximately independent of the transmitted torque, the expected efficiency would be 99.0% to 98.4%. This efficiency exceeds the state of the art over this speed range.

Author contact:

Justin J. Scheidler justin.j.scheidler@nasa.gov; Zachary A. Cameron zachary.a.cameron@nasa.gov; Thomas F. Tallerico thomas.tallerico@nasa.gov.

APPENDIX

This section contains the derivations for the uncertainty analysis that was conducted for the measurements obtained from NASA's E-Drives Rig. The uncertainty analysis is used to quantify the precision of the reported performance metrics.

Torque-based measurements (e.g., torque ripple) are governed only by the uncertainty of the torque transducers. However, mechanical efficiency is a calculated quantity that has a higher uncertainty due to error propagation. The uncertainty of the calculated efficiency U_η is quantified using the standard formula for the propagation of error (Ref. 11),

$$U_\eta = \pm \left[\sum_{g=1}^{N} \left(\left\{ \frac{\partial \eta}{\partial z_g} U_{z_g} \right\} \Big|_{z_g = \bar{z}_g} \right)^2 \right]^{1/2}, \tag{1}$$

where N is the number of measured quantities on which the calculated mechanical efficiency η depends and U_{z_g} is the uncertainty in the measured quantity z_g. In Eq. 1, the partial derivative and the uncertainty U_{z_g} are evaluated at the operating point $\bar{z}_g$. The mechanical efficiency is calculated as

$$\eta = \frac{P_\mathrm{o}}{P_\mathrm{i}} = \frac{T_\mathrm{o}\omega_\mathrm{o}}{T_\mathrm{i}\omega_\mathrm{i}}, \tag{2}$$

where P_o and P_i represent the output and input mechanical power, respectively, T_o and T_i denote the output and input torque, respectively, and ω_o and ω_i denote the output and input speed (in units of rad/s), respectively. The torque transducers installed in the E-Drives Rig provide measurements of not only the torque and speed but also the power. Inserting the first half of Eq. 2 into Eq. 1 one gets the efficiency uncertainty when the efficiency is calculated from the measured input and output mechanical power,

$$U_\eta = \pm \left[\left(\frac{1}{\bar{P}_\mathrm{i}} U_{P_\mathrm{o}} \big|_{P_\mathrm{o}=\bar{P}_\mathrm{o}} \right)^2 + \left(\frac{\bar{P}_\mathrm{o}}{\bar{P}_\mathrm{i}^2} U_{P_\mathrm{i}} \big|_{P_\mathrm{i}=\bar{P}_\mathrm{i}} \right)^2 \right]^{1/2}, \tag{3}$$

where U_{P_o} and U_{P_o} respectively are the uncertainty in the measured output and input power.

If instead the efficiency is calculated from the measured torques and speeds, the efficiency uncertainty is determined from the insertion of the second half of Eq. 2 into Eq. 1,

$$U_\eta = \pm \left[\left(\frac{\bar{\omega}_\mathrm{o}}{\bar{T}_\mathrm{i}\bar{\omega}_\mathrm{i}} U_{T_\mathrm{o}} \big|_{T_\mathrm{o}=\bar{T}_\mathrm{o}} \right)^2 + \left(\frac{\bar{T}_\mathrm{o}}{\bar{T}_\mathrm{i}\bar{\omega}_\mathrm{i}} U_{\omega_\mathrm{o}} \big|_{\omega_\mathrm{o}=\bar{\omega}_\mathrm{o}} \right)^2 + \left(\frac{\bar{T}_\mathrm{o}\bar{\omega}_\mathrm{o}}{\bar{T}_\mathrm{i}^2\bar{\omega}_\mathrm{i}} U_{T_\mathrm{i}} \big|_{T_\mathrm{i}=\bar{T}_\mathrm{i}} \right)^2 + \left(\frac{\bar{T}_\mathrm{o}\bar{\omega}_\mathrm{o}}{\bar{T}_\mathrm{i}\bar{\omega}_\mathrm{i}^2} U_{\omega_\mathrm{i}} \big|_{\omega_\mathrm{i}=\bar{\omega}_\mathrm{i}} \right)^2 \right]^{1/2}. \tag{4}$$

Equation 4 can be simplified by using the gear ratio GR of the magnetic gear, which relates the input and output quantities according to

$$GR = \frac{\omega_\mathrm{i}}{\omega_\mathrm{o}} = \frac{T_\mathrm{o}}{T_\mathrm{i}}. \tag{5}$$

Simplification of Eq. 4 using Eq. 5 gives

$$U_\eta = \pm \left[\left(\frac{U_{T_\mathrm{o}} \big|_{T_\mathrm{o}=\bar{T}_\mathrm{o}}}{\bar{T}_\mathrm{o}} \right)^2 + \left(\frac{U_{\omega_\mathrm{o}} \big|_{\omega_\mathrm{o}=\bar{\omega}_\mathrm{o}}}{\bar{\omega}_\mathrm{o}} \right)^2 + \left(\frac{U_{T_\mathrm{i}} \big|_{T_\mathrm{i}=\bar{T}_\mathrm{i}}}{\bar{T}_\mathrm{i}} \right)^2 + \left(\frac{U_{\omega_\mathrm{i}} \big|_{\omega_\mathrm{i}=\bar{\omega}_\mathrm{i}}}{\bar{\omega}_\mathrm{i}} \right)^2 \right]^{1/2}. \tag{6}$$

As expected, an increased uncertainty in any of the measured quantities increases the uncertainty in the calculated efficiency.

The uncertainty of the torque transducer's torque, speed, and power outputs are required to evaluate the efficiency uncertainties. The torque transducer's measurement uncertainties are calculated from the manufacturer's specifications according to a modified form of the design stage uncertainty U defined by Figliola and Beasley (Ref. 11),

$$U = k \left[u_0^2 + u_\mathrm{c}^2 \right]^{1/2}, \tag{7}$$

Table 2: Elemental measurement errors and resolution of the torque transducers used in the E-Drives Rig (Refs. 16, 17).

	Measured quantity			
	Torque (CAN bus)	Torque (frequency)	Speed	Power
Sensitivity tolerance[a,b]	-	$\pm 0.01\% \cdot T_{max}$	-	$\pm 0.01\% \cdot P_{rated}$
Linearity + hysteresis, for a max. torque in range:[c]				
0 to $0.2 \cdot T_{rated}$	$\pm 0.003\% \cdot 2T_{rated}$		-	$\pm 0.02 \cdot \omega/\omega_{rated}$
$> 0.2 \cdot T_{rated}$ to $0.6 \cdot T_{rated}$	$\pm 0.005\% \cdot 2T_{rated}$		-	$\pm 0.02 \cdot \omega/\omega_{rated}$
$> 0.6 \cdot T_{rated}$ to T_{rated}	$\pm 0.007\% \cdot 2T_{rated}$		-	$\pm 0.02 \cdot \omega/\omega_{rated}$
Temperature effect on output[d]	$\pm 0.02\% \cdot T_{max} \cdot (\Delta\Theta/10\ \mathrm{K})$		-	$\pm 0.05\% \cdot \omega/\omega_{rated} \cdot (\Delta\Theta/10\ \mathrm{K})$
Temperature effect on zero	$\pm 0.005\% \cdot T_{rated} \cdot (\Delta\Theta/10\ \mathrm{K})$		-	-
Repeatability[e]	$\pm 0.005\% \cdot T_{range}$		-	-
Effect of parasitic loads[f]	$\pm 0.2\% \cdot T_{rated} \cdot C_{load}$		-	$\pm 0.2\% \cdot P_{rated} \cdot C_{load}$
Resolution	-	$\pm 0.0008\% \cdot T_{rated}$	0.1 rpm	1 W
Instrument error	-	-	$\pm 0.00015\% \cdot \omega_{rated}$	-

[a]The reported values assume that the transducer's sensitivity is calibrated to an accuracy of $< \pm 0.01\%$ of T_{rated}.
[b]T_{max} is the absolute value of the maximum torque observed in a given test. P_{rated} is the rated power of the given torque transducer (i.e., $T_{rated} \cdot \omega_{rated}$)
[c]T_{rated} and ω_{rated} are the rated torque and speed (in units of rad/s), respectively, of the given torque transducer. In the E-Drives Rig, the torque transducer on the input (motor) side of the rig has ratings of 100 Nm and 22,000 rpm, whereas the torque transducer on the output (dynamometer) side of the rig has ratings of 100 Nm and 15,000 rpm.
[d]$\Delta\Theta$ is the maximum deviation of the torque transducer's temperature from the reference temperature.
[e]T_{range} is the full span of the torque observed in a given test.
[f]C_{load} is the combined ratio of the parasitic loads to the maximum allowable parasitic loads (i.e., C_{load} = (static axial force)/5 kN + (dynamic axial force)/2.5 kN + (static lateral force)/1 kN + (dynamic lateral force)/0.5 kN + (static bending moment)/50 Nm + (dynamic bending moment)/25 Nm).

where u_0 is the transducer's resolution error, which equals $\pm 0.5 \cdot$ resolution, u_c is the transducer's instrument error, and k is the coverage factor. The coverage factor specifies the confidence interval for the reported uncertainty (i.e., it defines the percentage of transducers whose actual uncertainty falls within the reported uncertainty). The coverage factor is essentially the number of standard deviations covered by the reported uncertainty. Here, a confidence level of 95% (coverage factor of 1.96) is used, which is standard practice (Ref. 11). The modifications are taken from the manufacturer's guidelines for uncertainty calculation. The instrument error depends on the transducer's elemental errors u_i according to

$$u_c = \left[\sum_{i=1}^{M} (d_i u_i)^2 \right]^{1/2}. \tag{8}$$

In Eq. 8, d_i is the distribution factor for the respective elemental error. The distribution factor converts the elemental error into a standard deviation. For error specifications that are valid for every transducer manufactured, the actual error of an individual transducer falls within a rectangular probability distribution with bounds given by the error specification; in this case, the distribution factor is $1/\sqrt{3}$ (≈ 0.58). For error specifications that are typical values, and individual transducer's actual error falls within a normal probability distribution with standard deviation equal to the specification; in this case, the distribution factor is 1. For the torque transducers used in the E-Drives Rig, only the specified repeatability error is a typical value. It should be noted that the manufacturer's calculations of the torque transducer's uncertainty don't consider the resolution error (i.e., they assume $U = u_c$). However, the resolution errors of the torque transducers used in the E-Drives Rig are very small; thus, they have a negligible effect on the design stage uncertainty (i.e., $U \approx u_c$). The elemental errors and resolution of the torque transducers used in the E-Drives Rig are summarized in Table 2.

ACKNOWLEDGMENTS

This work was supported by NASA's Revolutionary Vertical Lift Technology Project and NASA's Independent Research and Development Program.

REFERENCES

[1]Dixon, S. and Hall, C., *Fluid mechanics and thermodynamics of turbomachinery*, Elsevier, Inc., Waltham, MA, 7th edition, Ch. 5, 2014.

[2]Farokhi, S., *Aircraft propulsion*, John Wiley & Sons Ltd, West Sussex, United Kingdom, second edition, Ch. 4, 5, 7, 2014.

[3]Zhang, X., Bowman, C. L., O'Connell, T. C., and Haran, K. S., "Large electric machines for aircraft electric propulsion," *IET Electric Power Applications*, Vol. 12, (6), 2018, pp. 767–779.

[4]Anderson, A. D., Renner, N. J., Wang, Y., Agrawal, S., Sirimanna, S., Lee, D., Banerjee, A., Haran, K., Starr, M. J., and Felder, J. L., "System Weight Comparison of Electric Machine Topologies for Electric Aircraft Propulsion," 2018 AIAA/IEEE Electric Aircraft Technologies Symposium (EATS), 2018.

[5]Kish, J., "Sikorsky Aircraft Advanced Rotorcraft Transmission (ART) Program - Final Report," NASA-CR-191079, 1993.

[6]Heath, G., "Advanced Rotorcraft Transmission (ART) Program - Final Report," NASA-CR-191057, 1993.

[7]Uber, "eVTOL Vehicle Requirements and Missions," Available online, June 2018.

[8]Asnani, V., Scheidler, J., and Tallerico, T., "Magnetic gearing research at NASA," Proc. of AHS Intl. 74th Annual Forum, Phoenix, AZ, May 14–17, 2018.

[9]Scheidler, J. J., Asnani, V. M., and Tallerico, T. F., "NASA's Magnetic Gearing Research for Electrified Aircraft Propulsion," 2018 AIAA/IEEE Electric Aircraft Technologies Symposium (EATS), 2018.

[10]Anderson, A. D. and Asnani, V. M., "Concentric Magnetic Gearing: State of the Art and Empirical Trends," Technical report, NASA Technical Memorandum, In press.

[11]Figliola, R. and Beasley, D., *Theory and design for mechanical measurements*, John Wiley & Sons, Inc., Hoboken, NJ, fourth edition, 2015.

[12]Cameron, Z., Tallerico, T., and Scheidler, J., "Lessons Learned In Fabrication of High-Specific-Torque Concentric Magnetic Gear," Proc. of VFS 75th Annual Forum, Philadelphia, PA, May 13–16, 2019.

[13]Jian, L., Chau, K., Gong, Y., Jiang, J., Yu, C., and Li, W., "Comparison of coaxial magnetic gears with different topologies," *IEEE Transactions on Magnetics*, Vol. 45, (10), 2009, pp. 4526–4529.
doi: 10.1109/TMAG.2009.2021662

[14]Liu, X., Chau, K., Jiang, J., and Yu, C., "Design and analysis of interior-magnet outer-rotor concentric magnetic gears," *Journal of Applied Physics*, Vol. 105, (7), 2009, pp. 07F101.
doi: 10.1063/1.3058619

[15]Matthee, A., Gerber, S., and Wang, R.-J., "A high performance concentric magnetic gear," Proc. of 23rd Southern African Universities Power Engineering Conference, Johannesburg, South Africa, 2015.
doi: 10.13140/RG.2.1.1493.6167

[16]HBM, "T12HP Data Sheet," Available online [https://www.hbm.com/en/6384/t12hp-torque-transducer-with-maximum-precision/], 2019.

[17]HBM, "Webinar: the calculation of the measurement uncertainty for torque applications," Available online [https://www.hbm.com/en/3941/the-calculation-of-the-measurement-uncertainty-for-torque-applications/], 2019.